

On the Importance of Lennard–Jones Parameter Calibration in QM/MM Framework: Reaction Path Tracing via Free Energy Gradient Method for Ammonia Ionization Process in Aqueous Solution

Yoshiyuki Koyano,[1] Norio Takenaka,[1] Yukinori Nakagawa,[1] and Masataka Nagaoka*[1,2]

[1]Graduate School of Information Science, Nagoya University, Furo-cho, Chikusa-ku, Nagoya 464-8601

[2]JST-CREST

Received November 16, 2009; E-mail: mnagaoka@is.nagoya-u.ac.jp

The free energy gradient (FEG) method combined with the QM/MM–MD calculation has realized full-atomic structural optimization of the solute NH_3–H_2O molecule pair in aqueous solution, exploring successful tracing of the reaction path on the free energy surface from the neutral state (H_3N–H_2O) to the ionized (H_4^+N–O^-H) through the transition state ($H_3N\cdots H^+\cdots O^-H$). To reproduce accurately the structural change of the hydrated molecule pair, the LJ parameter calibration in the QM/MM nonelectrostatic interaction was essential for four kinds of QM solute species, i.e., OH^-, H_2O, NH_3, and NH_4^+, treated in the NDDO-SSRP framework with the ab initio quality. Two linear interpolations of these calibrated LJ parameters optimized at the NSS and ISS were utilized in the path-dependent FEG calculation, as is common in the free energy perturbation treatment. After including the effects of the intramolecular entropic contribution and quantum tunneling, the free energies of activation and reaction were satisfactorily estimated to be 13.8 and 9.8 kcal mol^{-1} (1 kcal = 4.184 kJ), respectively. It is expected that far more agreement with the experimental values should be reasonably attained if the QM region were extended to three surrounding water molecules to take in the electron delocalization effect adequately.

Solution reaction always involves a variety of interactions among not only solute species but also a large number of solvent molecules. In those theoretical studies on such reaction systems, the quantum mechanical/molecular mechanical (QM/MM) method[1–3] combined with molecular dynamics (MD) or Monte Carlo (MC) calculation has been becoming one of the prevailing approaches, since it is suitable to treat precisely the solute electronic state under the explicit influence of instantaneous configurations of the surrounding solvent molecules.

In the QM/MM system, a solute species or a complex including a few solvent molecules around it, that is, a solvated complex, is described quantum mechanically. The chemical accuracy in QM/MM calculations depends strongly on description of the QM subsystem. Since ab initio QM representations have been shown to provide good chemical accuracy in studies on gas-phase reactions of small molecules, a number of studies on solution reactions have been attempted using ab initio QM/MM–MD or –MC calculations. In many of them, approximate treatments have been introduced to manage the great computational cost of the QM calculation. For example, the averaged solvent electrostatic potential/molecular dynamics (ASEP/MD) method[4] was applied successfully to such solution reaction systems where the instantaneous solvent polarization might not influence seriously the reaction. On the other hand, for the purpose of executing direct QM/MM–MD calculation, low-cost semiempirical QM methods with the neglect of diatomic differential overlap (NDDO) approximation,[5] i.e., AM1[6] and PM3[7] method, were widely adopted to describe systems in the QM theoretical level. However, they lead sometimes to inaccurate description in hydrogen-bonded systems and the proton transfers. For the purpose of applications to such phenomena in solution, we have recently proposed the NDDO method with specific solution reaction parameters (SSRP),[8] in which the charge distribution is to be improved significantly by reference to ab initio molecular orbital (MO) calculations. Furthermore, the method combined with the method adapted for intermolecular studies (MAIS), i.e., the NDDO–MAIS–SSRP method, was shown to provide good results for the solute NH_3–H_2O molecule pair, which was modeled as the essential reactant system in the ammonia ionization reaction in aqueous solution.[9]

In addition, the parameterization of the QM/MM intermolecular interaction has been recently recognized as one of the important issues in modeling solution reaction systems. In fact, Tu and Laaksonen modified the Lennard–Jones (LJ) parameter set to reproduce the intermolecular interaction for a water dimer at ab initio Hartree–Fock level and applied it to MD calculation of a QM H_2O "solute" in aqueous solution.[10] As a result, the interaction energy between solute and solvent was found too weak because the non-additive effects were neglected in the parameterization. Further, to reproduce the hydrated structure and thermodynamic characteristics of solutes in solution, Martín et al. proposed an iterative optimization procedure of the LJ parameters[11] and as a demonstration, the optimization for a QM H_2O solute in aqueous solution was executed by the use of direct ab initio QM/MM–MD method and ASEP/MD method.[4] Nevertheless, in most studies of the QM/MM–MD calculation on solution reactions,[12,13] the LJ

Published on the web April 29, 2010; doi:10.1246/bcsj.20090296

parameters in the QM/MM nonelectrostatic interaction have been taken directly from the conventional MM force fields. If the QM/MM intermolecular interaction were adjusted to reproduce the structural and energetic characteristics of the hydrated solute species at the reactant state, it is doubtful that it might bring about a reliable description at the product state as well. Thus, the LJ parameters in the QM/MM intermolecular interaction should be determined far more carefully.

In the present study, taking into consideration those previous studies, we take the ammonia ionization reaction in aqueous solution. The QM/MM nonelectrostatic interaction has been parameterized to reproduce justifiably the hydrated structure change of the solute NH_3–H_2O molecule pair during the ionization. By using the free energy gradient (FEG) method[14–20] combined with the QM/MM–MD calculation, we have executed the full-atomic structural optimizations of the solute molecule pair for the ionization process in solution and explored the reaction path on the free energy surface (FES).

This article is organized as follows: first, in the following section, (i) QM/MM–MD method, (ii) optimization of Lennard–Jones parameters in QM/MM nonelectrostatic interaction, and (iii) free energy gradient method are explained. In the third section, results and discussion are made with respect to (i) radial distribution function and hydration enthalpy, (ii) free energy profile on NH_3 ionization reaction in aqueous solution, and (iii) hydrated structure of solute NH_3–H_2O molecule pair. Finally, the present study is summarized in concluding remarks.

Theory and Method

QM/MM–MD Method. In hybrid QM/MM–MD method,[1–3] the effective Hamiltonian of the total system, $\hat{H}_{\mathrm{eff}}$, is described as the sum of the following three terms;

$$\hat{H}_{\mathrm{eff}} = \hat{H}_{\mathrm{QM}} + \hat{H}_{\mathrm{QM/MM}} + \hat{H}_{\mathrm{MM}} \tag{1}$$

where $\hat{H}_{\mathrm{QM}}$ and $\hat{H}_{\mathrm{MM}}$ are the terms of the QM and the MM subsystem, respectively. In the present study, a solute molecule was treated as the QM subsystem and MM solvent H_2O molecules were represented by the rigid TIP3P model.[21] The QM/MM interaction term $\hat{H}_{\mathrm{QM/MM}}$ is defined as a sum of electrostatic and nonelectrostatic interaction energy between the QM solute and MM solvent molecules;

$$\hat{H}_{\mathrm{QM/MM}} = \hat{H}^{\mathrm{elec}}_{\mathrm{QM/MM}} + \hat{H}^{\mathrm{vdW}}_{\mathrm{QM/MM}} \tag{2}$$

where the superscript vdW is conventionally used for the nonelectrostatic term.[22] The electrostatic interaction energy is expressed as

$$\hat{H}^{\mathrm{elec}}_{\mathrm{QM/MM}} = \sum_M q_M V_{\mathrm{QM}}(\mathbf{R}_M) \tag{3}$$

where q_M is the Mth atomic point charge located at the position $\mathbf{R}_M$ in the MM solvent H_2O molecule and $V_{\mathrm{QM}}(\mathbf{R}_M)$ is the sum of electrostatic potential generated by the electrons and nucleus in the QM subsystem. The second term in the right-hand side of eq 2 is described as a sum of LJ type functions,

$$\hat{H}^{\mathrm{vdW}}_{\mathrm{QM/MM}} = \sum_A \sum_M \varepsilon_{AM} \left\{ \left(\frac{R^{\mathrm{e}}_{AM}}{R_{AM}} \right)^{12} - 2 \left(\frac{R^{\mathrm{e}}_{AM}}{R_{AM}} \right)^{6} \right\} \tag{4}$$

where R_{AM} is the distance between the Ath QM and the Mth MM atoms, and ε_{AM} and R^{e}_{AM} are a couple of LJ parameters for the Ath QM atom interacting with the Mth MM atom. This is not only the conventional exchange repulsive and van der Waals interaction terms but also the correction term to the electrostatic and hydrogen-bonding interactions. The present definition of electrostatic potential $V_{\mathrm{QM}}(\mathbf{R}_M)$ of the QM subsystem is the standard one implemented in the ROAR 2.1 module[23] of the MD simulation program package AMBER 7.0.[24] The details of the definition are obtained in our previous papers.[8,9] The total system potential energy V is thus expressed as follows,

$$V = \langle \Psi | \hat{H}_{\mathrm{QM}} + \hat{H}_{\mathrm{QM/MM}} | \Psi \rangle + V_{\mathrm{MM}} \tag{5}$$

$$= V_{\mathrm{SB}} + V_{\mathrm{MM}} \tag{6}$$

where $|\Psi\rangle$ denotes an instantaneous SCF wave function of solute electrons, and V_{SB} is the instantaneous eigenvalue and is the sum of both the solute potential energy and the interaction energy between the solute and solvent.

For the QM Hamiltonian $\hat{H}_{\mathrm{QM}}$, we have adopted an optimum strategy using semiempirical MO method with NDDO approximation with specific solution reaction parameters (SSRP).[8] In optimization of LJ parameters in the QM/MM nonelectrostatic interaction, four kinds of QM solute species (OH^-, H_2O, NH_3, and NH_4^+) were described by the PM3-SSRP method[8] and were improved to reproduce significantly the potential energy surface (PES) around the equilibrium states and the charge distributions of solute species by reference to ab initio MO calculation obtained at the MP2/6-31+G(d,p) level. Further, in calculating the free energy (FE) profile in aqueous solution, the PM3–MAIS–SSRP method[9] was employed to a couple of molecules, i.e., a QM solute NH_3–H_2O molecule pair, so as to reproduce satisfactorily the PES and the charge-transfer process for the NH_3 ionization reaction.

For the whole system including a QM solute molecule and 241 TIP3P H_2O molecules treated molecular mechanically, QM/MM–MD calculations were carried out in a cubic simulation box ($19.34 \times 19.34 \times 19.34\,\text{Å}^3$) under the periodic boundary condition. The mass density in the box was prepared to be ca. $1.000\,\mathrm{g\,cm^{-3}}$. For the geometry constraint of solvent TIP3P molecules, the velocity-Verlet algorithm was used with the SHAKE and RATTLE schemes.[25] The simultaneous equations of motion were numerically solved with a time step 2.0 fs and the non-bonded cutoff distance 9.0 Å. After equilibration, sampling run was executed for 30000 steps and was used to calculate physical quantities by averaging over this equilibrium sampling. The temperature was kept at 300 K with the Nosé–Hoover chain algorithm[26] and the system was maintained to be a canonical (*NVT*) ensemble.

Optimization of Lennard–Jones Parameters in QM/MM Nonelectrostatic Interaction. In this subsection, the optimization procedure of the LJ parameters is explained in the QM/MM nonelectrostatic interaction energy (eq 4). For the purpose of reproducing the hydrated structure of the QM solute NH_3–H_2O molecule pair not only at the neutral stable state (NSS) but also the ionized stable state (ISS), a couple of LJ parameters of the QM solute interacting with the MM solvent H_2O molecule were determined for four solute species (OH^-, H_2O, NH_3, and NH_4^+), respectively. The LJ parameters for O–OW and N–OW in the neutral species (H_2O and NH_3) are

adopted as those of the QM solute NH_3–H_2O molecule pair at the NSS, and the parameters in the ionized species (OH^- and NH_4^+) are used for the solute NH_4^+–H_2O ion pair at the ISS. OW is the abbreviation of the oxygen atoms of the MM solvent H_2O molecule.

Inspired by the proposal on the optimization procedure in solution by Martín et al.,[11] we here adopted a procedure with some modifications in semiempirical QM/MM framework. We explored a couple of LJ parameters, i.e., ε_{AM} and R^{e}_{AM}, by finding the minimal value of the following evaluation function $F(\varepsilon_{AM},R^{\mathrm{e}}_{AM})$:

$$F(\varepsilon_{AM}, R^{\mathrm{e}}_{AM}) = \frac{\{E^{\mathrm{calc}}_{\mathrm{hyd}}(\varepsilon_{AM}, R^{\mathrm{e}}_{AM}) - E^{\mathrm{exp}}_{\mathrm{hyd}}\}^2}{w_E^2} + \frac{\{r^{\mathrm{RDF,calc}}_{1\mathrm{st}}(\varepsilon_{AM}, R^{\mathrm{e}}_{AM}) - r^{\mathrm{RDF,exp}}_{1\mathrm{st}}\}^2}{w_r^2} \quad (7)$$

where E_{hyd} is the hydration enthalpy of the QM solute and $r^{\mathrm{RDF}}_{1\mathrm{st}}$ is the first peak position in the radial distribution function (RDF) between their heavy atoms of the QM solute and MM solvent molecules. In eq 7, the superscripts "calc" and "exp" mean the calculated value and experimental one, respectively. In the present study, the calculated value of E_{hyd} was obtained as an average value of the solute–solvent interaction energy, following a lot of previous work where the same convention was adopted since the strict estimation of E_{hyd} requires much computational cost to consider the solvent reorganization effect caused by the solute insertion. Both w_E and w_r being the weight parameters of the hydration enthalpy and the first peak position in the RDF, we generated systems for many pairs of LJ parameters (ε_{AM},R^{e}_{AM}) by varying them by $\Delta\varepsilon_{AM} = 0.05$ Å and $\Delta R^{\mathrm{e}}_{AM} = 0.05\,\mathrm{kcal\,mol^{-1}}$, respectively. By executing MD calculations for these pairs of LJ parameters, we obtained the optimized LJ parameters. For an initial pair (ε_{AM},R^{e}_{AM}), a successive of direct QM/MM–MD calculations have been executed to estimate the following 8 numbers of differences, $\Delta F(\pm\Delta\varepsilon_{AM},0)$, $\Delta F(0,\pm\Delta R^{\mathrm{e}}_{AM})$, $\Delta F(\pm\Delta\varepsilon_{AM},\pm\Delta R^{\mathrm{e}}_{AM})$, and $\Delta F(\pm\Delta\varepsilon_{AM},\mp\Delta R^{\mathrm{e}}_{AM})$, defined as follows.

$$\Delta F(\pm\Delta\varepsilon_{AM}, 0) = F(\varepsilon_{AM} \pm \Delta\varepsilon_{AM}, R^{\mathrm{e}}_{AM}) - F(\varepsilon_{AM}, R^{\mathrm{e}}_{AM}) \quad (8)$$

$$\Delta F(0, \pm\Delta R^{\mathrm{e}}_{AM}) = F(\varepsilon_{AM}, R^{\mathrm{e}}_{AM} \pm \Delta R^{\mathrm{e}}_{AM}) - F(\varepsilon_{AM}, R^{\mathrm{e}}_{AM}) \quad (9)$$

$$\Delta F(\pm\Delta\varepsilon_{AM}, \pm\Delta R^{\mathrm{e}}_{AM}) = F(\varepsilon_{AM} \pm \Delta\varepsilon_{AM}, R^{\mathrm{e}}_{AM} \pm \Delta R^{\mathrm{e}}_{AM}) - F(\varepsilon_{AM}, R^{\mathrm{e}}_{AM}) \quad (10)$$

$$\Delta F(\pm\Delta\varepsilon_{AM}, \mp\Delta R^{\mathrm{e}}_{AM}) = F(\varepsilon_{AM} \pm \Delta\varepsilon_{AM}, R^{\mathrm{e}}_{AM} \mp \Delta R^{\mathrm{e}}_{AM}) - F(\varepsilon_{AM}, R^{\mathrm{e}}_{AM}) \quad (11)$$

For the present increments ($\Delta\varepsilon_{AM}$,$\Delta R^{\mathrm{e}}_{AM}$), the typical ratio

$$\frac{\Delta F(\Delta\varepsilon_{AM}, 0)}{\Delta F(0, \Delta R^{\mathrm{e}}_{AM})} \cong 5 \quad (12)$$

and therefore the weight parameters w_E and w_r were taken to be 5 and 1, respectively.

For the LJ parameters used in the treatment by the free energy perturbation (FEP) theory[27] for the ionization process in solution, we have introduced the following linear interpolation of those at the NSS and ISS. The LJ parameters between solute NH_3 and solvent H_2O, i.e., $\varepsilon_{\mathrm{N1–OW}}$ and $R^{\mathrm{e}}_{\mathrm{N1–OW}}$, are defined as a function of the distance for N1–H5, $R_{\mathrm{N1–H5}}$, by using those at the NSS, $\varepsilon^{\mathrm{neu}}_{\mathrm{N1–OW}}$ and $R^{\mathrm{e,neu}}_{\mathrm{N1–OW}}$, and for the ISS, $\varepsilon^{\mathrm{ion}}_{\mathrm{N1–OW}}$ and $R^{\mathrm{e,ion}}_{\mathrm{N1–OW}}$,

$$\begin{cases} \varepsilon_{\mathrm{N1–OW}} = \dfrac{R^{\mathrm{ion}}_{\mathrm{N1–H5}} - R_{\mathrm{N1–H5}}}{R^{\mathrm{ion}}_{\mathrm{N1–H5}} - R^{\mathrm{neu}}_{\mathrm{N1–H5}}}\varepsilon^{\mathrm{neu}}_{\mathrm{N1–OW}} + \dfrac{R_{\mathrm{N1–H5}} - R^{\mathrm{neu}}_{\mathrm{N1–H5}}}{R^{\mathrm{ion}}_{\mathrm{N1–H5}} - R^{\mathrm{neu}}_{\mathrm{N1–H5}}}\varepsilon^{\mathrm{ion}}_{\mathrm{N1–OW}} & (13) \\ R^{\mathrm{e}}_{\mathrm{N1–OW}} = \dfrac{R^{\mathrm{ion}}_{\mathrm{N1–H5}} - R_{\mathrm{N1–H5}}}{R^{\mathrm{ion}}_{\mathrm{N1–H5}} - R^{\mathrm{neu}}_{\mathrm{N1–H5}}}R^{\mathrm{e,neu}}_{\mathrm{N1–OW}} + \dfrac{R_{\mathrm{N1–H5}} - R^{\mathrm{neu}}_{\mathrm{N1–H5}}}{R^{\mathrm{ion}}_{\mathrm{N1–H5}} - R^{\mathrm{neu}}_{\mathrm{N1–H5}}}R^{\mathrm{e,ion}}_{\mathrm{N1–OW}} & (14) \end{cases}$$

where $R^{\mathrm{neu}}_{\mathrm{N1–H5}}$ and $R^{\mathrm{ion}}_{\mathrm{N1–H5}}$ are the N1–H5 interatomic distances at the NSS and ISS, their values being set to 1.722 and 1.024 Å, respectively. In the same way, LJ parameters between solute H_2O and solvent H_2O, i.e., $\varepsilon_{\mathrm{O6–OW}}$ and $R^{\mathrm{e}}_{\mathrm{O6–OW}}$, are described as a function of the distance for H5–O6, $R_{\mathrm{H5–O6}}$, by using those for the NSS, $\varepsilon^{\mathrm{neu}}_{\mathrm{O6–OW}}$ and $R^{\mathrm{e,neu}}_{\mathrm{O6–OW}}$, and for the ISS, $\varepsilon^{\mathrm{ion}}_{\mathrm{O6–OW}}$ and $R^{\mathrm{e,ion}}_{\mathrm{O6–OW}}$,

$$\begin{cases} \varepsilon_{\mathrm{O6–OW}} = \dfrac{R^{\mathrm{ion}}_{\mathrm{H5–O6}} - R_{\mathrm{H5–O6}}}{R^{\mathrm{ion}}_{\mathrm{H5–O6}} - R^{\mathrm{neu}}_{\mathrm{H5–O6}}}\varepsilon^{\mathrm{neu}}_{\mathrm{O6–OW}} + \dfrac{R_{\mathrm{H5–O6}} - R^{\mathrm{neu}}_{\mathrm{H5–O6}}}{R^{\mathrm{ion}}_{\mathrm{H5–O6}} - R^{\mathrm{neu}}_{\mathrm{H5–O6}}}\varepsilon^{\mathrm{ion}}_{\mathrm{O6–OW}} & (15) \\ R^{\mathrm{e}}_{\mathrm{O6–OW}} = \dfrac{R^{\mathrm{ion}}_{\mathrm{H5–O6}} - R_{\mathrm{H5–O6}}}{R^{\mathrm{ion}}_{\mathrm{H5–O6}} - R^{\mathrm{neu}}_{\mathrm{H5–O6}}}R^{\mathrm{e,neu}}_{\mathrm{O6–OW}} + \dfrac{R_{\mathrm{H5–O6}} - R^{\mathrm{neu}}_{\mathrm{H5–O6}}}{R^{\mathrm{ion}}_{\mathrm{H5–O6}} - R^{\mathrm{neu}}_{\mathrm{H5–O6}}}R^{\mathrm{e,ion}}_{\mathrm{O6–OW}} & (16) \end{cases}$$

where $R^{\mathrm{neu}}_{\mathrm{H5–O6}}$ and $R^{\mathrm{ion}}_{\mathrm{H5–O6}}$ are given as the H5–O6 interatomic distances at the NSS and ISS, their values being 1.027 and 2.047 Å, respectively.

In addition, QM/MM–MD calculations using conventional LJ parameters in the MM force field were executed in order to compare the results for the LJ parameters optimized in the present study. The LJ parameters for the TIP3P H_2O model[21] are adopted as those for O–OW between the QM solute H_2O and MM TIP3P H_2O molecules. As the LJ parameters for N–OW, those between the OPLS model for NH_3[28] and TIP3P model for H_2O are determined by using the Lorentz–Berthelot combination rule.[29]

Free Energy Gradient Method. We developed the free energy gradient (FEG) method with application to identify the optimized structure of the solute molecule in solution.[14–20] Being analogous to the energy gradient method on the Born–Oppenheimer PES in ab initio MO theory, the FEG method utilizes the force on the FES to search minima or reaction path on the FES.

In equilibrium, the ensemble average of an observable is to be replaced as the time average calculated over an MD trajectory, provided the trajectory is ergodic. Then, the force on the FES, $\mathbf{F}^{\mathrm{FE}}(\mathbf{q}^{\mathrm{S}})$, is equal to the time average of the forces acting on each atom of the solute NH_3–H_2O molecule pair with the geometry $\mathbf{q}^{\mathrm{S}}$.

$$\mathbf{F}^{\mathrm{FE}}(\mathbf{q}^{\mathrm{S}}) = -\frac{\partial A(\mathbf{q}^{\mathrm{S}})}{\partial \mathbf{q}^{\mathrm{S}}} = -\left\langle \frac{\partial V_{\mathrm{SB}}(\mathbf{q}^{\mathrm{S}})}{\partial \mathbf{q}^{\mathrm{S}}} \right\rangle \quad (17)$$

where the Helmholtz free energy $A(\mathbf{q}^S)$ is a function of not only thermodynamic variables (N, V, T) but also the solute structure $\mathbf{q}^S$. The brackets denote the equilibrium ensemble average

$$\langle \cdots \rangle = \frac{\int d\mathbf{q}^B (\cdots) \exp(-\beta V(\mathbf{q}^S))}{\int d\mathbf{q}^B \exp(-\beta V(\mathbf{q}^S))} \quad (18)$$

where $\mathbf{q}^B$ denotes the solvent coordinates as a whole, and V is the potential energy of the whole system (eq 5). By the FEP theory,[27] the FE difference at an optimization step i, ΔA_i, is described as follows.

$$\Delta A_i = A_{i+1} - A_i = -k_B T \ln\langle \exp[-\beta\{V_{SB}(\mathbf{q}^S_{i+1}) - V_{SB}(\mathbf{q}^S_i)\}]\rangle_i \quad (19)$$

where $\mathbf{q}^S_i$ and $\mathbf{q}^S_{i+1}$ are solute structures at optimization step i and $i+1$, respectively. The subscript i in the average $\langle \cdots \rangle_i$ in eq 19 means that the average is taken over the sampling at $\mathbf{q}^S_i$. By applying the steepest descent scheme,[30] the optimization cycle was repeated for the FEP treatment, until the following condition, i.e., the zero gradient condition, is satisfied.

$$\left\langle \frac{\partial V_{SB}(\mathbf{q}^s)}{\partial \mathbf{q}^s} \right\rangle_i \approx 0 \quad (20)$$

Results and Discussion

Radial Distribution Function and Hydration Enthalpy. According to the optimization procedure mentioned above, we determined the LJ parameters in the QM/MM nonelectrostatic interaction for four kinds of QM solute species, i.e., OH^-, H_2O, NH_3, and NH_4^+. To demonstrate the reproducibility of structural and energetic characteristics of hydrated complexes for these solute species, both r^{RDF}_{1st}, the first peak positions in the RDF for the QM solute interacting with MM solvent molecules and E_{hyd}, the hydration enthalpies of the QM solute, were obtained (Table 1) by the QM/MM–MD calculation using two sets of the LJ parameters (ε_{AM},R^e_{AM}), i.e., the parameter set optimized in the present study and that for MM force field.

First, we discuss these results for two neutral solute species, H_2O and NH_3 molecules. From some previous experiments,[32–35] the first peak position in the O–OW RDF for H_2O molecule in aqueous solution was 2.8 Å and the hydration enthalpy for H_2O was -9.9 kcal mol^{-1}, while for NH_3 molecule the first peak position in the N–OW RDF was 2.8 Å and the hydration enthalpy was -7.9 kcal mol^{-1}. These reports indicate that by using the presently optimized LJ parameter set, the theoretically calculated values of both the first peak positions and the hydration enthalpies for H_2O and NH_3 molecule were able to reproduce quite well the corresponding experimental ones (Table 1). In contrast, by using the LJ parameter set of a conventional MM force field, the first peak in the O–OW RDF for H_2O is found located at a slightly longer position than that in the experiment by 0.2 Å. For H_2O, the calculated value of hydration enthalpy was less stabilized than the experimental value by 1.4 kcal mol^{-1}. Similarly, for NH_3, the first peak position of in the N–OW RDF shifted to longer distance by 0.3 Å and the calculated hydration enthalpy was found unstabilized by 1.9 kcal mol^{-1}. These observations suggest that among these neutral H_2O or NH_3 molecules (QM solute) and the surrounding H_2O molecules (MM solvent), the nonelectrostatic interactions using the presently optimized LJ parameter set should work considerably better as the correction for the electrostatic interactions.

Table 1. LJ Parameter Sets in the QM/MM Nonelectrostatic Interaction Energy between Solute O (or N) and Solvent OW Atoms Optimized for the Present Study and the MM Force Field, together with the First Peak Positions of the RDF and the Hydration Enthalpies for Four Solute Species (H_2O, NH_3, OH^-, and NH_4^+) in Aqueous Solution

	Lennard–Jones parameters for QM solute–MM solvent		r^{RDF}_{1st} /Å	E_{hyd} /kcal mol^{-1}
	ε_{AM} /kcal mol^{-1}	R^e_{AM} /Å		
O–OW				
H_2O				
MM force field	0.15	3.54	3.0	−8.5
present	0.20	3.45	2.8	−9.9
expt.	—	—	2.8	−9.9
OH^-				
MM force field	0.15	3.54	2.8	−84.3
present	6.40	2.30	2.4	−115.7
expt.	—	—	(2.3)[a)]	−116.2
N–OW				
NH_3				
MM force field	0.16	3.69	3.1	−6.0
present	0.20	3.30	2.8	−8.0
expt.	—	—	2.8	−7.9
NH_4^+				
MM force field	0.16	3.69	2.8	−63.7
present	3.90	3.20	3.1	−89.3
expt.	—	—	3.1	−88.8

a) Empirical potential structure refinement (EPSR) procedure (Ref. 31).

Next, we discuss the results for two solute OH^- and NH_4^+ ions. Since there is no experimental data for the RDF of OH^- ion interacting with H_2O molecules (O–OW), instead, the first peak position in the RDF (2.3 Å) by the empirical potential structure refinement (EPSR) procedure[31] was taken as the reference value. The experimental value of hydration enthalpy for OH^- ion was -116.2 kcal mol^{-1}.[36] For NH_4^+ ion, the first peak position in the N–OW RDF was reported to be 3.1 Å[37] and the hydration enthalpy was -88.8 kcal mol^{-1}.[36] By using the optimized LJ parameters, these calculated values for OH^- and NH_4^+ ions were found in quite good agreement with the corresponding experimental ones (Table 1). On the other hand, by using the conventional MM force field parameters, the first peak in the O–OW RDF for OH^- appeared remarkably longer than the experimental one by 0.5 Å. The hydration enthalpy for OH^- ion was -84.3 kcal mol^{-1} and found considerably unstabilized compared to the experimental value by 31.9 kcal mol^{-1}. The first peak position in the N–OW RDF for NH_4^+ ion shifted to shorter distance by 0.3 Å and the hydration

enthalpy was less stabilized than that by the experiment by 25.1 kcal mol^{-1}. From these results, it was found that the naïve use of the conventional MM force field parameters in the QM/MM nonelectrostatic interactions should be inappropriate to reproduce structural and energetic characteristics of hydrated complexes for a number of solute species, especially for such ions as OH^- and NH_4^+. This is natural because these original LJ parameters were almost calibrated to these atoms in neutral species, i.e., H_2O and NH_3 molecule.

In the optimized LJ parameter set, the radius R^e_{AM} for OH^- and NH_4^+ ions shifted to shorter distances than those for H_2O and NH_3 molecules by 1.15 and 0.10 Å, and the depth ε_{AM} for OH^- and NH_4^+ became quite larger than those for H_2O and NH_3 by 6.20 and 3.70 kcal mol^{-1}, respectively (Table 1). It was found that the values of LJ parameters optimized for solute ionized species were greatly different from those for neutral species. By using only one pair of LJ parameters for O–OW and N–OW, it might be difficult to reflect the hydrated structure change of the solute NH_3–H_2O molecule pair accompanying the ionized reaction. Therefore, we have prepared the LJ parameter sets (ε_{AM},R^e_{AM}) for the QM solute NH_3–H_2O molecule pair at two stable states, i.e., NSS and ISS, and have combined them as functions of the distance O–OW and N–OW, linearly interpolating as eqs 13–16.

Free Energy Profile of NH_3 Ionization Reaction in Aqueous Solution. To evaluate the FEs of activation and reaction for ammonia ionization process in aqueous solution, the FE profiles have been computed as a function of the distance between the transferring proton H5 and the donor oxygen atom O6, i.e., $R_{H5–O6}$, in the range from 1.027 to 2.077 Å by 0.03 Å increment, optimizing all other geometric parameters of the solute NH_3–H_2O molecule pair by using the FEG method. The resultant FE profile in solution is shown as closed circles (●) and open ones (○) in Figure 1. The former is the FE profile obtained by using the present LJ parameter set interpolated for those optimized at the NSS and ISS (Set I), while the latter is that using the parameter set of MM force fields (Set II). In addition, the potential energy (PE) profile in gas phase is also drawn by a broken curve (- - -) in Figure 1.

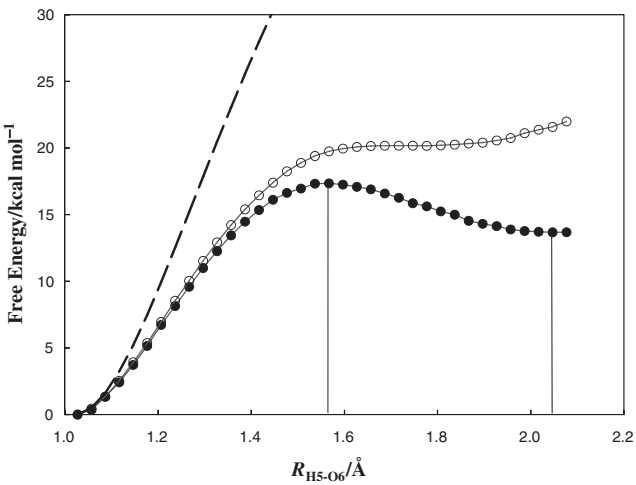

Figure 1. FE profiles for the ammonia ionization reaction in aqueous solution using the interpolated LJ parameter set (Set I, closed circles: ●) and those of the conventional MM force field set (Set II, open circles: ○) along the reaction coordinate $R_{H5–O6}$ by the FEG method. The broken curve shows the potential energy profile along the same structural change in gas phase.

In the distance $R_{H5–O6}$ between 1.1 and 1.4 Å, we observed similar monotonic increases in both FE profiles, whose slopes are more gentle than that of the PE profile in gas phase. This means that in aqueous solution large hydration energy offsets the destabilization of the solute PE. However, in the region $R_{H5–O6} > 1.4$ Å, the shapes of two FE profiles characteristically change, depending clearly on the difference between the LJ parameter sets adopted in the QM/MM nonelectrostatic interaction. It is verified that there exist clearly TS and ISS on the FE profile for Set I (●). Although in the region $R_{H5–O6} > 1.6$ Å, the FE profile for Set II (○) is almost flat to 1.9 Å without the TS observation. For Set I, the TS corresponds to the maximum on the FE profile at $R_{H5–O6} = 1.567$ Å, while the ISS is a local minimum located at $R_{H5–O6} = 2.047$ Å. Then the FEs of activation and reaction for Set I are 17.3 and 13.7 kcal mol^{-1}, respectively. By using the interpolated LJ parameter set (Set I), it was concluded that the FE profile should reproduce reasonably better characteristics of the ionization process of ammonia in aqueous solution.

The free-energetic contributions from intramolecular motion of the solute NH_3–H_2O molecule pair and the quantum tunneling of the transferring proton are absent from the present calculated values. As a matter of fact, through the Hessian matrix calculations at the solute geometries at the NSS, TS, and ISS,[14] the former contribution was estimated from the vibrational frequency analysis, while the latter was by the empirical correction formula of the quantum tunneling.[38,39] By taking these two contributions into consideration, the FEs of activation and reaction are corrected to be 13.8 and 9.8 kcal mol^{-1}, respectively. On the other hand, since the experimental values for the FEs of activation and reaction were estimated to be 9.57[40] and 6.48 kcal mol^{-1},[41] respectively, there exists still a slight difference between the theoretical and experimental values in the FEs of activation and reaction, that is, 4.23 and 3.32 kcal mol^{-1}, respectively.

We consider here the difference in the FEs. It is generally acknowledged that the chemical accuracy in the QM/MM calculation depends strongly on description of the QM subsystem at the MO theoretical level. Since in the present study the PM3–MAIS–SSRP method[9] was adopted to the solute NH_3–H_2O molecule pair treated as the QM subsystem, the resultant intermolecular electrostatic interactions and the proton-transfer process in the QM solute molecule pair could be reproduced satisfactorily at almost the same quality as the ab initio MP2/6-31+G(d,p) level. Nevertheless, the FE profile using the conventional LJ parameter set of MM force field (Set II) did not show even qualitatively the experimental result. Therefore, for Set I, it would be said that the characteristic difference between the theoretical and experimental values in the FEs must be responsible essentially for the inaccurate description in the QM/MM nonelectrostatic interactions. It is true that in the present optimization of the LJ parameters the solvent reorganization effect caused by solute species, especially for such ions as OH^- and NH_4^+, could be a non-negligible contribution to the hydration enthalpy E_{hyd}. How-

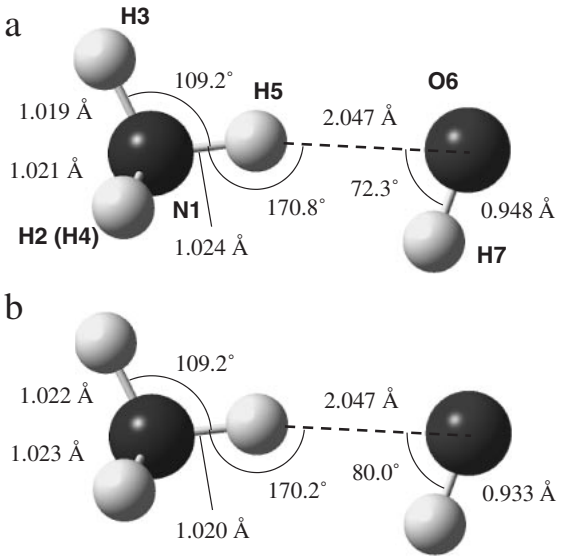

Figure 2. Optimized structures of the solute NH_3–H_2O molecule pair at $R_{H5–O6} = 2.047$ Å in aqueous solution, using (a) the interpolated LJ parameter set (Set I) and (b) those of the conventional MM force field (Set II).

ever, due to the high computational cost, it is a hard work to fit the hydration enthalpy correctly by including the solvent reorganization effect. Thus, it can be reasonably expected that the agreement in the present FEs of activation and reaction with the experimental ones would become much better by more quantitative fitting of the hydration enthalpy. In the next subsection, we will discuss the remaining difference in the FEs, originating in the hydrated structure of the solute NH_3–H_2O molecule pair.

Hydrated Structure of Solute NH_3–H_2O Molecule Pair. In the vicinity of the ionized state, the shape of the FE profile depends clearly on the difference in the LJ parameters, as shown in the preceding subsection. For Set I and II, the optimized structures of the solute NH_3–H_2O molecule pair at the reaction coordinate $R_{H5–O6} = 2.047$ Å (more appropriately, the solute NH_4^+–OH^- ion pair) are shown in Figure 2. In all of the geometric parameters, those for Set I are almost coincident with those for Set II except for the angle $\theta_{H5–O6–H7}$, whose difference between for Set I and II shows 7.7 degree. The decrease of $\theta_{H5–O6–H7}$ for Set I is easily explained by MD snapshots of the hydrated solute OH^- ion (Figure 3). For Set I, the hydroxy oxygen atom forms 3 hydrogen bonds with 3 surrounding solvent water molecules to maintain the tetrahedral structure and all of the lengths of the hydrogen bonds are shorter than the distance H5–O6 of 2.047 Å (Figure 3a).

It is supportive that, in the Car-Parrinello MD calculation of the OH^- ion in aqueous solution, Tuckerman et al. observed two characteristic hydrated complexes, i.e., the $(H_7O_4)^-$ and $(H_9O_5)^-$ complexes, whose hydroxy oxygen atoms are coordinated with 3 and 4 H_2O molecules, respectively.[42] The hydrated structure of the present OH^- ion for Set I corresponds to the former $(H_7O_4)^-$ complex, although it was found slightly distorted from the ideal tetrahedral one. This is because the accessible orientation of the approaching solvent H_2O molecules is restricted by the presence of the NH_4^+ ion near the

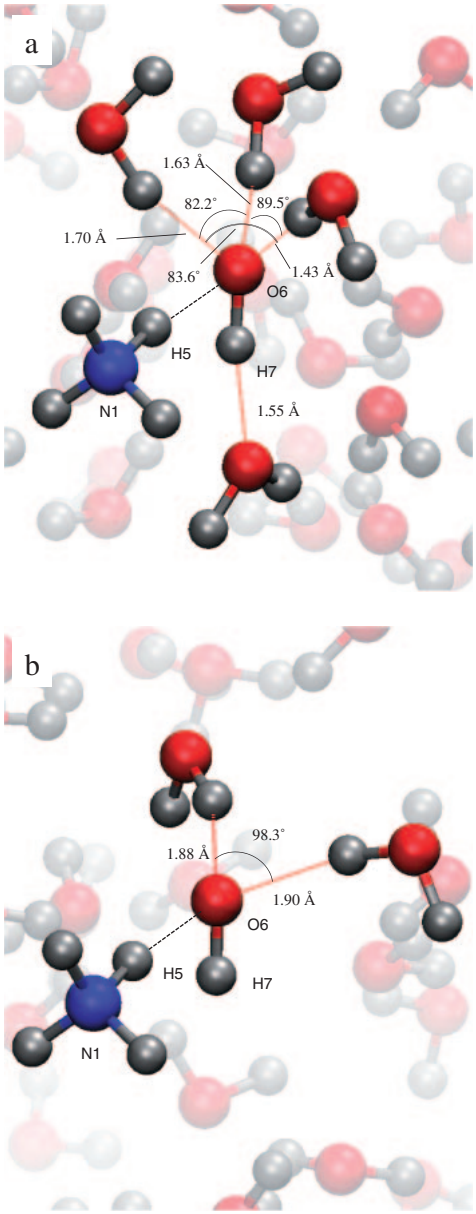

Figure 3. MD snapshots of the solute NH_3–H_2O molecule pair and the solvent H_2O hydrogen bonds with the OH^- ion at $R_{H5–O6} = 2.047$ Å, using (a) the interpolated LJ parameter set (Set I) and (b) those of the conventional MM force field (Set II).

OH^- ion, not only for just the steric hindrance but also for weakening of mutual repulsion among 3 lone electron pairs of the oxygen of OH^-. In contrast, for Set II, the hydrated structure of OH^- ion is rather similar to that of a hydrated H_2O molecule forming 2 hydrogen bonds via 2 lone electron pairs, and the lengths of the hydrogen bonds (1.85 and 1.97 Å) are longer than those for Set I (Figure 3b), which is reasonable because Set II was optimized literally for these atoms of neutral species, as mentioned previously.

Thus, it is clearly noticed that there exists obvious difference between the hydrated structures for Set I and II, although intramolecular geometric parameters of the solute NH_3–H_2O molecule pair in solution at $R_{H5–O6} = 2.047$ Å are almost

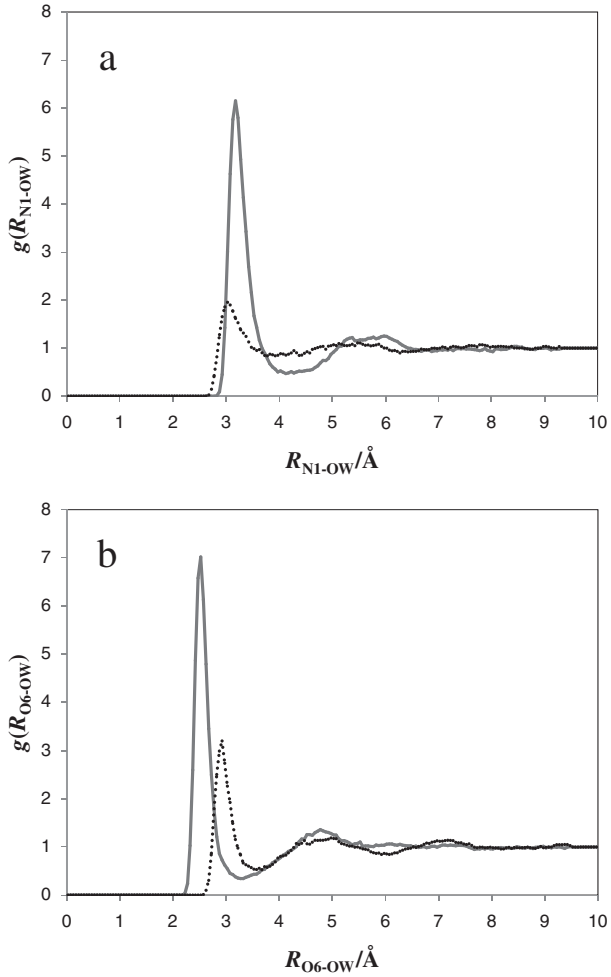

Figure 4. RDFs of the solvent OW atoms around the N1 or O6 atoms of the solute NH_3–H_2O molecule pair at $R_{H5\text{–}O6} = 2.047$ Å using the interpolated LJ parameter set (Set I, solid curve) and the MM force field set (Set II, broken curve) as the functions of the distances $R_{N1\text{–}OW}$ (a) and $R_{O6\text{–}OW}$ (b).

independent of the LJ parameters in the QM/MM nonelectrostatic interactions among solute and solvent molecules. The RDFs with respect to the solute–solvent intermolecular distances N1–OW and O6–OW at $R_{H5\text{–}O6} = 2.047$ Å are shown in Figure 4. As a result, at $R_{H5\text{–}O6} = 2.047$ Å for Set I, we observed the clear enhancement of the first peak in the N1–OW RDF, which shifted to a fair longer distance to 3.2 Å (Figure 4a). Moreover, the minima for Set I and II between the first and second peaks in the N1–OW RDF were located at 4.2 and 3.8 Å, respectively. Thus, the size of the first hydration shell of the NH_4^+ ion for Set I can be recognized to become larger than that for Set II. Also, as shown in Figure 4b, the clear enhancement of the first peak in the O6–OW RDF was observed at $R_{H5\text{–}O6} = 2.047$ Å for Set I and the position in the O6–OW RDF for Set I (2.5 Å) shifted to a shorter distance than that for Set II (2.9 Å). However, the shapes and characteristics of the O–OW RDF for both Set I and II appear almost the same in the region $R_{O6\text{–}OW} > 3.7$ Å. Therefore, it is understood that some solvent H_2O molecules forming hydrogen bonds with the OH^- ion are locating at the same time in the first hydration shell of the NH_4^+ ion. In other words, the clear enhancements of both peaks in the N1–OW and O6–OW RDFs for Set I at $R_{H5\text{–}O6} = 2.047$ Å (Figure 3), in comparison to those for Set II, are understood to be originating in the effective number increase of the hydrogen bonds connecting to the QM oxygen of the solute NH_4^+–OH^- molecule (or ion) pair.

Table 2. ESP Atomic Charges of the Solute NH_3–H_2O Molecule Pair in Aqueous Solution at the Reaction Coordinate $R_{H5\text{–}O6} = 1.027$, 1.567, and 2.047 Å Using the Interpolated LJ Parameter Set (Set I) and the MM Force Field Set (Set II)

	Present (Set I)			MM force field (Set II)		
$R_{H5\text{–}O6}$/Å:	1.027	1.567	2.047	1.027	1.567	2.047
N1	−0.667	−0.839	−0.602	−0.659	−0.862	−0.639
H2	0.258	0.394	0.396	0.255	0.394	0.403
H3	0.276	0.406	0.389	0.272	0.408	0.393
H4	0.258	0.394	0.396	0.255	0.394	0.403
H5	0.406	0.578	0.423	0.405	0.587	0.439
O6	−0.941	−1.334	−1.451	−0.937	−1.295	−1.347
H7	0.410	0.400	0.449	0.410	0.374	0.348

The above observation is further supported by the charge distribution of the solute molecule pair. The ESP atomic charge distributions at $R_{H5\text{–}O6} = 1.027$, 1.567, and 2.047 Å are shown in Table 2. At $R_{H5\text{–}O6} = 1.027$ Å (the neutral NH_3–H_2O molecule pair), the ESP charge difference on all of the atoms between Set I and II were just within 0.008 *e*. Similarly, even at $R_{H5\text{–}O6} = 2.047$ Å (the NH_4^+–OH^- ion pair), each atomic charge on the NH_4^+ ion for Set I and II, shows almost the same value, expecting no positive role to enhance the number of hydrogen bonds. On the other hand, there exist considerable differences for O6 and H7 atoms, i.e., −0.104 and 0.101 *e*, respectively, which should be notified as the principal origin of both enhancements of the first peaks in the N1–OW and O6–OW RDFs for Set I.

In the relation of the hydrated structure with the LJ parameters, the distance between the solute and the nearest-neighbor solvent molecules decreases with decrease of R_{AM}^{e}, while the probability of existence at the distance R_{AM}^{e} increases with increase of ε_{AM}. Thus, it is a matter of course that the hydrated structure of the OH^- ion changes by the significant modification of the LJ parameters for O–OW and its change should be influenced by the electronic polarization in the OH^- ion and vice versa. It is then clear that the destabilization due to the charge polarization in the hydrated solute OH^- ion for Set I was compensated by the stabilization by 3 hydrogen atoms of the surrounding H_2O molecules (Figures 3 and 4). In relation, in our preceding paper, where the hydration process of an NH_3 molecule from the vapor phase to the aqueous liquid phase was investigated using QM/MM–MD calculation, it was then indicated that the explicit description of QM polarization of even a solute NH_3 molecule is essentially important to reproduce the FE of hydration.[43] Thus, also in NH_4^+ in aqueous solution, it is expected that far more agreement of the present values of FEs of activation and reaction with the experimental ones should be reasonably attained if the QM region were extended to 3 surrounding water molecules to take in the electron delocalization effect adequately.

Concluding Remarks

In this article, by the FEG method combined with the QM/MM–MD calculation, we realized the reaction path tracing on the FES, on which full-atomic structural optimizations were executed for the solute NH_3–H_2O molecule pair at the NSS (H_3N–H_2O), TS (H_3N···H^+···O^-H) and ISS (H_4^+N–O^-H). To reproduce accurately the hydrated structure change of the solute NH_3–H_2O molecule pair in aqueous solution, using the LJ parameters in the QM/MM nonelectrostatic interaction optimized previously for four kinds of QM solute species, i.e., OH^-, H_2O, NH_3, and NH_4^+, the effective LJ parameters of the oxygen and the nitrogen in the solute molecule pair (or the solute ion pair) were expressed by two linear interpolations between those of OH^- and H_2O and between those of NH_3 and NH_4^+.

In the case that the LJ parameters of the conventional MM force field (Set II) were adopted for the FEG calculation, both the TS and the ISS were not observed. In contrast, in the FE profile calculated using the present interpolated LJ parameters (Set I), there exists clearly the TS ($R_{H5–O6} = 1.567$ Å) and the ISS ($R_{H5–O6} = 2.047$ Å) and the resultant FEs of activation and reaction were estimated to be 13.8 and 9.8 kcal mol^{-1}, respectively, whose values include the entropic effect of intramolecular motion of the solute molecule pair and the quantum tunneling effect of the transferring proton. It is true that the agreement with the experimental values might be not satisfied since the latter were estimated to be 9.57 and 6.48 kcal mol^{-1}. However, it is expected that the present treatment would become reasonably improved to be in far more agreement with the experimental values if the QM region were extended to include three surrounding water molecules so as to take in the electron delocalization effect adequately.

Being concerned with the structural characteristics, in the RDFs with respect to the solute–solvent intermolecular distances of N1–OW and O6–OW, the clear enhancements of both peaks at $R_{H5–O6} = 2.047$ Å were observed for Set I, in comparison to those for Set II, and are understood as the effective number increase of the hydrogen bonds connecting to the QM oxygen of the solute pair. Finally, it is concluded that the structural and energetic characteristics of the hydrated complex, i.e., the solute and surrounding solvent molecules as a whole, could depend strongly on the LJ parameters in the QM/MM nonelectrostatic interaction although the intramolecular structural parameters of the solute NH_3–H_2O molecule pair themselves might be almost independent of the LJ parameters.

This work was supported by a Grant-in-Aid for Science Research from the Ministry of Education, Culture, Sports, Science and Technology (MEXT) in Japan, and also by the Core Research for Evolutional Science and Technology (CREST) "High Performance Computing for Multi-scale and Multi-physics Phenomena" from the Japan Science and Technology Agency (JST).

References

1 A. Warshel, M. Levitt, *J. Mol. Biol.* **1976**, *103*, 227.
2 U. C. Singh, P. A. Kollman, *J. Comput. Chem.* **1986**, *7*, 718.
3 M. J. Field, P. A. Bash, M. Karplus, *J. Comput. Chem.* **1990**, *11*, 700.
4 M. L. Sanchez, M. A. Aguilar, F. J. Olivares del Valle, *J. Comput. Chem.* **1997**, *18*, 313.
5 J. A. Pople, D. P. Stantry, G. A. Segal, *J. Chem. Phys.* **1965**, *43*, S129.
6 M. J. S. Dewar, E. G. Zoebisch, E. F. Healy, J. J. P. Stewart, *J. Am. Chem. Soc.* **1985**, *107*, 3902.
7 J. J. P. Stewart, *J. Comput. Chem.* **1989**, *10*, 209.
8 N. Takenaka, Y. Koyano, Y. Nakagawa, M. Nagaoka, *J. Comput. Chem.* **2010**, *31*, 1287.
9 Y. Koyano, N. Takenaka, Y. Nakagawa, M. Nagaoka, *J. Comput. Chem.* **2010**, in press.
10 Y. Tu, A. Laaksonen, *J. Chem. Phys.* **1999**, *111*, 7519.
11 M. E. Martín, M. A. Aguilar, S. Chalmet, M. F. Ruiz-López, *Chem. Phys.* **2002**, *284*, 607.
12 G. Vayner, K. N. Houk, W. L. Jorgensen, J. I. Brauman, *J. Am. Chem. Soc.* **2004**, *126*, 9054.
13 M. Valiev, B. C. Garrett, M.-K. Tsai, K. Kowalski, S. M. Kathmann, G. K. Schenter, M. Dupuis, *J. Chem. Phys.* **2007**, *127*, 051102.
14 N. Okuyama-Yoshida, M. Nagaoka, T. Yamabe, *Int. J. Quantum Chem.* **1998**, *70*, 95.
15 M. Nagaoka, N. Okuyama-Yoshida, T. Yamabe, *J. Phys. Chem. A* **1998**, *102*, 8202.
16 N. Okuyama-Yoshida, M. Nagaoka, T. Yamabe, *J. Phys. Chem. A* **1998**, *102*, 285.
17 N. Okuyama-Yoshida, K. Kataoka, M. Nagaoka, T. Yamabe, *J. Chem. Phys.* **2000**, *113*, 3519.
18 H. Hirao, Y. Nagae, M. Nagaoka, *Chem. Phys. Lett.* **2001**, *348*, 350.
19 Y. Nagae, Y. Oishi, N. Naruse, M. Nagaoka, *J. Chem. Phys.* **2003**, *119*, 7972.
20 M. Nagaoka, Y. Nagae, Y. Koyano, Y. Oishi, *J. Phys. Chem. A* **2006**, *110*, 4555.
21 W. L. Jorgensen, J. Chandrasekhar, J. D. Madura, R. W. Impey, M. L. Klein, *J. Chem. Phys.* **1983**, *79*, 926.
22 F. J. Luque, N. Reuter, A. Cartier, M. F. Ruiz-López, *J. Phys. Chem. A* **2000**, *104*, 10923.
23 A. Cheng, R. S. Stanton, J. J. Vincent, A. van der Vaart, K. V. Damodaran, S. L. Dixon, D. S. Hartsough, M. Mori, S. A. Best, G. Monard, M. Garcia, L. Van Zant, K. M. Merz, Jr., *ROAR 2.1*, The Pennsylvania State University, **2002**.
24 D. A. Case, D. A. Pearlman, J. W. Caldwell, T. E. Cheatham, III, J. Wang, W. S. Ross, C. L. Simmerling, T. A. Darden, K. M. Merz, R. V. Stanton, A. L. Cheng, J. J. Vincent, M. Crowley, V. Tsui, H. Gohlke, R. J. Radmer, Y. Duan, J. Pitera, I. Massova, G. L. Seibel, U. C. Singh, P. K. Weiner, P. A. Kollman, *AMBER 7*, University of California, San Francisco, **2002**.
25 S. Miyamoto, P. A. Kollman, *J. Comput. Chem.* **1992**, *13*, 952.
26 G. J. Martyna, M. L. Klein, M. Tuckerman, *J. Chem. Phys.* **1992**, *97*, 2635.
27 R. W. Zwanzig, *J. Chem. Phys.* **1954**, *22*, 1420.
28 R. C. Rizzo, W. L. Jorgensen, *J. Am. Chem. Soc.* **1999**, *121*, 4827.
29 M. P. Allen, D. J. Tildesley, *Computer Simulation of Liquids*, Oxford University Press, Oxford, **1987**.
30 M. Levitt, S. Lifson, *J. Mol. Biol.* **1969**, *46*, 269.
31 S. Imberti, A. Botti, F. Bruni, G. Cappa, M. A. Ricci, A. K. Soper, *J. Chem. Phys.* **2005**, *122*, 194509.

32 A. K. Soper, F. Bruni, M. A. Ricci, *J. Chem. Phys.* **1997**, *106*, 247.
33 G. Hura, J. M. Sorenson, R. M. Glaeser, T. Head-Gordon, *J. Chem. Phys.* **2000**, *113*, 9140.
34 A. H. Narten, *J. Chem. Phys.* **1968**, *49*, 1692.
35 A. Ben-Naim, Y. Marcus, *J. Chem. Phys.* **1984**, *81*, 2016.
36 C. E. Klots, *J. Phys. Chem.* **1981**, *85*, 3585.
37 G. Pálinkás, T. Radnai, G. I. Szász, K. Heinzinger, *J. Chem. Phys.* **1981**, *74*, 3522.
38 J. I. Steinfeld, J. S. Francisco, W. L. Hase, *Chemical Kinetics and Dynamics*, Prentice Hall, Englewood Cliffs, New Jersey, **1989**.
39 I. Shavitt, *J. Chem. Phys.* **1959**, *31*, 1359.
40 S. L. Friess, E. S. Lewis, A. Weissberger, *Technique of Organic Chemistry, Investigation of Rates and Mechanisms of Reactions*, Interscience, New York, **1963**, Vol. 8-II.
41 D. D. Perrin, *Ionisation Constants of Inorganic Acids and Bases in Aqueous Solution*, 2nd ed., Pergamon, Oxford, **1982**.
42 M. Tuckerman, K. Laasonen, M. Sprik, M. Parrinello, *J. Phys. Chem.* **1995**, *99*, 5749.
43 N. Takenaka, Y. Koyano, M. Nagaoka, *Chem. Phys. Lett.* **2010**, *485*, 119.